ISSN 0208-7774 TRIBOLOGIA 4/2022 p. 85–94
DOI: 10.5604/01.3001.0016.1616

Mirosław SZALA*, Tadeusz HEJWOWSKI**

CAVITATION EROSION RESISTANCE OF HIGH-ALLOYED FE-BASED WELD HARDFACINGS DEPOSITED VIA SMAW METHOD

ODPORNOŚĆ NA EROZJĘ KAWITACYJNĄ WYSOKOSTOPOWYCH TWARDYCH POWŁOK NAPAWANYCH NA OSNOWIE ŻELAZA WYTWORZONYCH METODĄ SMAW

Key words: cavitation erosion, hard facing, pad welding, wear mechanism, roughness, hardness.

Abstract: In order to investigate the cavitation erosion (CE) resistance of high-alloyed ferrous hardfacings, the three different deposits were pad welded by the shielded metal arc welding (SMAW) method. Consumable electrodes differed in the content of carbide-forming elements, and pad welds were deposited onto the S235JR structural. The CE tests, conducted according to ASTM G32 standard, indicated that hardfacings reveal lower mass loss than the reference stainless steel AISI 304 (X5CrNi18-10). The hardfacings show increasing resistance to CE in the following order: Cr-C < Cr-C-Mo < Cr-C-Mo-V-W. The reference steel revealed more than twenty times higher material loss in the CE test than Cr-C-Mo-V-W hardfacing, which had outstanding hardness (825HV0.3). The profilometric measurements and scanning electron microscopy investigations showed large changes in valley and peak sizes of the roughness profiles for materials which displayed high erosion rates. The erosion mechanism of the coatings can be classified as brittle-ductile and relies on cracking, chunk removal of material, pits and craters formation, and deformation of fractured material tips and edges. Hardfacing materials failed primarily due to brittle fractures with different severities. Specimen surface degradation follows the changes in Ra, Rz, Rv, and Rp roughness parameters and well-corresponds to the proposed roughness rate (RR) parameter.

Słowa kluczowe: erozja kawitacyjna, napawanie utwardzające, mechanizm zużycia, chropowatość, twardość.

Streszczenie: W celu zbadania odporności na erozję kawitacyjną (EK) wysokostopowych napoin na osnowie żelaza napawano trzema materiałami metodą SMAW. Elektrody otulone różniły się zawartością pierwiastków węglikotwórczych. Napoiny wykonano na stali konstrukcyjnej S235JR. Testy EK, przeprowadzone zgodnie z normą ASTM G32, wykazały niższy ubytek masy napoin w porównaniu do referencyjnej stali odpornej na korozję AISI 304 (X5CrNi18-10). Napoiny wykazują rosnącą odporność na EK w następującej kolejności: Cr-C < Cr-C-Mo < Cr-C-Mo-V-W. Referencyjna próbka stalowa wykazała w teście EK ponad dwudziestokrotnie większy ubytek materiału niż napoina Cr-C-Mo-V-W, która miała wyjątkowo wysoką twardość (825HV0.3). Pomiary profilometryczne i badania przeprowadzone przy użyciu skaningowego mikroskopu elektronowego wykazały duże zmiany wielkości dolin i szczytów profilu chropowatości dla materiałów wykazujących wysoką szybkość erozji. Mechanizm EK powłok można sklasyfikować jako krucho-plastyczny i opiera się na pękaniu, usuwaniu kawałków materiału, tworzeniu wgłębień i kraterów oraz deformacji pękniętych fragmentów kraterów oraz deformacji wyodrębnionych szczytów i krawędzi materiału. Napawany materiał podlega niszczeniu przez jego pękanie w różnym nasileniu. Degradacja powierzchni próbek pogłębia się wraz ze zmianą parametrów chropowatości Ra, Rz, Rv i Rp i dobrze koresponduje z proponowanym parametrem RR (zmiana chropowatości pow. degradowanej).

* ORCID 0000-0003-1059-8854 Department of Materials Engineering, Faculty of Mechanical Engineering, Lublin University of Technology, Nadbystrzycka 36D, 20-618 Lublin, Poland; m.szala@pollub.pl.
** ORCID 0000-0002-4254-4562 Department of Materials Engineering, Faculty of Mechanical Engineering, Lublin University of Technology, Nadbystrzycka 36D, 20-618 Lublin, Poland; t.hejwowski@pollub.pl.

INTRODUCTION

An important stage of regenerating hydro-components is choosing the appropriate reclamation method and additional materials. Usually, the deposited coatings should combine high corrosion resistance with high resistance to erosion by solid particle laden fluid and cavitation erosion (CE). Many researchers systematically investigate the anti-erosive performance of various material systems fabricated using surface engineering or welding methods **[L. 1]**. For example, thermal spraying has been considered by many researchers as a promising technology for improving the CE resistance of metal substrates **[L. 2**–4**]**, and from a broad range of coating materials, hard cermet of WC-Co and WC-CoCr types show the most promising CE results **[L. 5–8]**. Although many advanced methods, such as PVD coating deposition or ion implantation **[L. 9–11]**, are considered to minimalise cavitation erosion, the welding methods still seem the most effective **[L. 12–14]**. Zhao et al. **[L. 15]** investigated the cavitation erosion/corrosion synergy and wear behaviours of nickel-based weld overlays deposited by cold metal transfer. It was revealed that deposited Inconel 625 and Hastelloy C-276 coatings show erosion rate of AISI 304 substrate exceeds those reported for welds, even though the hardness of the reference stainless steel and nickel overlays were at a comparable level. In work **[L. 16]**, authors claim that NiCrBSi weld overlays deposited via oxy-acetylene welding show superior CE resistance to AISI 304 stainless steel and cast iron. On the other hand, the CE behaviour of coatings cannot be strictly referred to as sole hardness dependent, especially in the case of complex microstructures such as high-alloyed alloys or metal matrix composites (MMC). For example, Duraiselvam et al. **[L. 17]** showed a positive effect of applying laser-clad from nickel aluminide intermetallic composites and matrix composites with TiC reinforcement on the CE resistance of AISI 420 steel. Contrary to that, Szymański et al. **[L. 18]** showed that the fabrication of a TiC-rich layer on cast steel and cast iron improves wear behaviour but deteriorates the CE resistance of fabricated composites. The differences in weld hardfacing microstructures strongly influenced CE results. Furthermore, Fedorov et al. **[L. 19]** claim that high-alloyed chromium steels are highly suitable for preventing components from CE. On the other hand, advanced welding techniques such as laser cladding and plasma transferred arc (PTA) methods give promising anti-CE results, but their application for in-field regeneration is difficult. Therefore, classic arc welding, such as the shielded metal arc welding (SMAW) method, is recommended. Available consumable electrodes allow the production of a broad range of alloy compositions of pad welds and obtain different hardness, microstructures and satisfactory operational performance in specific environments. SMAW is a favourable welding method enabling the deposition of a wide range of high-alloyed consumable electrodes onto industrial components of complex shapes, especially in hard-to-access locations.

Hardness is generally considered the predominant factor in determining the anti-wear performance of hardfacings, although the overlays' microstructure should also be considered. The microstructure of pad welds derives from the fabrication method, post-processing (heat treatment), and mainly from the chemical composition of feedstock materials. This paper shows the CE performance of hardfacings containing various contents of alloying elements such as carbon, chromium, molybdenum, manganese, silicon, vanadium and tungsten. There is scarce information available in the literature regarding the CE resistance of high-alloyed Fe-based weld hardfacings. Therefore, the analysed set of materials was selected to obtain pad welds with different hardness and to fill a gap in the knowledge of the CE performance of iron-based pad welds. Thus this study aimed to compare the effect of hardness on the CE resistance of SMAW hardfacings and the hardfacings CE behaviour with this reference AISI 304 stainless steel.

MATERIALS AND METHODS

Hardfacings characterisation and research methods

The paper compares the cavitation erosion (CE) behaviour of three welded hardfacings with the reference stainless steel. The investigated materials' characterisation is shown in **Table 1**. The 10 mm thick structural steel substrate grade S235JR pad was welded using the SMAW method. Three layers of each material were deposited on the substrate plate to achieve the nominal chemical composition of the consumable electrode, and

Table 1. Specimens codes, the content of main chemical elements, and nominal hardness
Tabela 1. Kody próbek, zawartość głównych pierwiastków chemicznych i twardość nominalna

Sample name	Sample characterisation	A chemical element, wt%					As-welded metal hardness
		C	Cr	Mn	Si	Other	
AISI 304	X5CrNi18-10, steel plate	<0.07	17.5–19.5	<2	<1	Ni 8-10.5%; Nmax 0.11	Substrate nominal hardness 210 HB
Cr-C	Hardfacing, electrode OK 84.52	0.25	13	0.5	0.5	–	49–55 HRC
Cr-C-Mo	Hardfacing electrode, OK 83.50	0.4	6	0.5	0.4	0.6% Mo	50–60 HRC
Cr-C-Mo-V-W	Hardfacing electrode, OK 85.65	0.93	4.7	1.4	1.4	Mo 7.3%, V 1.6%, W 1.39%	59–61 HRC

then the samples assigned to CE testing were cut and machined by grinding to obtain the surface roughness of Ra < 0,17 µm, Rz < 1,42 µm Rp < 0,56 µm and Rv <0.86 µm. The description of electrode applications is given in the supplier's datasheets **[L. 20]**. The OK 84.52 general-purpose electrode produces a corrosion-resistant, fully martensitic steel deposit. The electrode is suitable for hard facing shafts, racks and pinions, links and pins, valve seats of cast steel, mixer arms, feed gear, knives, loading buckets and track rollers, the OK 83.50 is a hard facing electrode for the repair welding of worn parts of agricultural equipment, forestry tools, loading machines and alike, and the OK 85.65 is a hard facing electrode which gives the high-speed steel deposit applied in repair welding of cutting tools, drills, stamping machines etc. The diameter of consumable electrodes equals 3.2 mm, and the employed welding current is approx. of 130A. According to the knowledge of the authors, these hardfacings have not been CE investigated. The obtained results were compared with those for AISI 304 (X5CrNi18-10) reference steel specimens cut from the 10 mm thick plate. This stainless-steel grade is a popular reference material used in different experiments. The surface hardness of the hardfacings has been investigated using the Vickers method and EN-ISO 6507-1 standard using the load of 2.942 N (HV0.3) and 10 s dwelling time. At least ten indentations were made to obtain statistical accuracy.

The CE resistance tests were carried out following the ASTM G32 standard **[L. 21]**. The sonotrode tip distance from the sample was 0.5 mm ± 0.05 mm, and the medium in which cavitation was induced was distilled water, see **Figure 1**. The analysis of the resistance to CE consisted of systematic measurements of the weight loss of the tested samples with an accuracy of 0.01 mg. In the current study, the total exposure time lasted 6 hours. The test rig used in the study has been described in the previous paper **[L. 22]**. The eroded surfaces were examined using the surface profiler (Surtronic S-128, Taylor-Hobson, Leicester, UK) according to the ISO 4287 standard. SEM (Scanning Electron Microscopy) analyses of damaged surfaces were carried out to reveal the failure mechanism of eroded surfaces.

Moreover, the introduced in the previous paper **[L. 23]** expression for the roughening rate, RR has been employed, see equation (1). It allows for the characterisation of the entire roughness of cavitation-eroded surfaces. RR factor combines the width (RSm), height (Rt) of the roughness profile and mean roughness (Ra) parameters vs the specific exposure time (t).

$$\mathrm{RR(t)} = \frac{RSm(t)\cdot[Ra(t)-Ra_{t0}]}{Rt(t)},\ \mu m \qquad (1)$$

RR gives information about CE surface damage and also can be related to the kinetics of the CE mechanism.

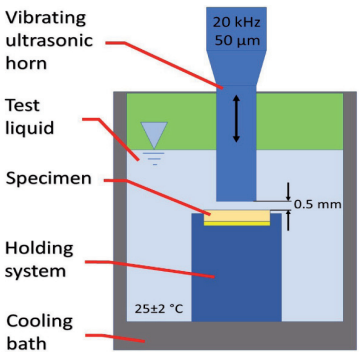

Fig. 1. Schematic representation of the ultrasonic vibratory system used for cavitation testing
Rys. 1. Schemat urządzenia ultradźwiękowego użytego w badaniach kawitacyjnych

RESULTS AND DISCUSSION

A hardness comparison of reference stainless steel and hardfacings is shown in **Figure 2**. The deposited hardfacings have a high hardness at the level of hardened steels, which is in accord with the data provided by the manufacturer **[L. 20]**, see **Table 1**. The 627-825 HV0.3 hardness of pad welds corresponds with the hardness reported for high alloyed martensitic and tool steel and hardfacings of that type **[L. 24, 25]**. The stainless steel hardness agrees with values reported in the CE literature **[L. 26]**. Of course, the high hardness of pad welds derives from the alloying elements such as carbon, chromium, manganese, and molybdenum content which are responsible for the formation of martensite and hard phases such as different types of carbides during the thermal welding cycle **[L. 27–29]**. Hardness is one of the most important material properties responsible for the anti-wear and erosion resistance of materials. The CE resistance has been widely correlated with hardness, however, this relationship works well for a group of similar engineering materials such as structural steels **[L. 30]** or stainless steels **[L. 31]**, and hardness alone cannot be considered an indicator of erosion resistance in the case of multiphase materials **[L. 16, 17]**. Cavitation erosion (CE) mass loss and erosion rate plots are presented in **Figure 3**. In our work, while comparing the information given in **Figure 2** and **Figure 3**, it seems that the hardness of three hardfacings correlates with CE results, i.e., high hardness facilitates CE resistance **Figure 4a**.

CE plots (**Figure 3**) show that the cavitation resistance of hardfacings increased in the following order: Cr-C < Cr-C-Mo < Cr-C-Mo-V-W. The erosion rate of reference stainless steel (approx. 6.49 mg/h) exceeds three times this found for Cr-C hard facing. The Cr-C-Mo-V-W hard facing, which shows superior resistance to CE, exhibits a constant and the lowest erosion rate of 0.32 mg/h. All hard facing present lower erosion rates than those previously reported for cast iron and cast steel **[L. 18]**, ceramic **[L. 32]**, and metallic **[L. 33]** coatings and are comparable to WC-Co type cermet coatings **[L. 8]** and higher than HIPed Stellite 6 **[L. 34]**. This corresponds to the lowest erosion surface damage revealed by the profilometric (**Figs. 4, 5**) and SEM (**Fig. 6**) investigations. The highest roughness values, **Figure 4b**, were noted for severely damaged AISI 304 steel. The roughness of eroded samples shows a trend to a correlation with

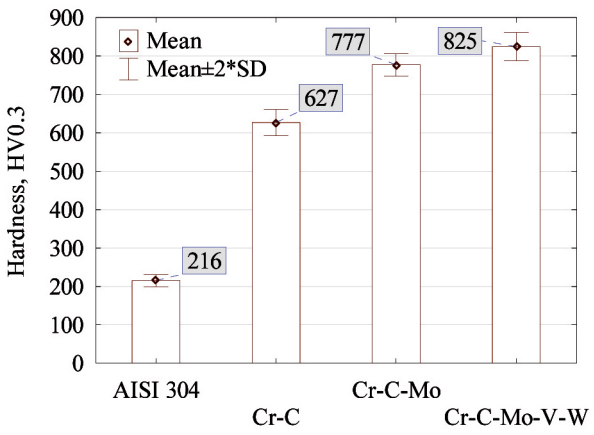

Fig. 2. Hardness of the reference stainless steel and hard facing layers
Rys. 2. Twardość referencyjnej stali nierdzewnej i napoin

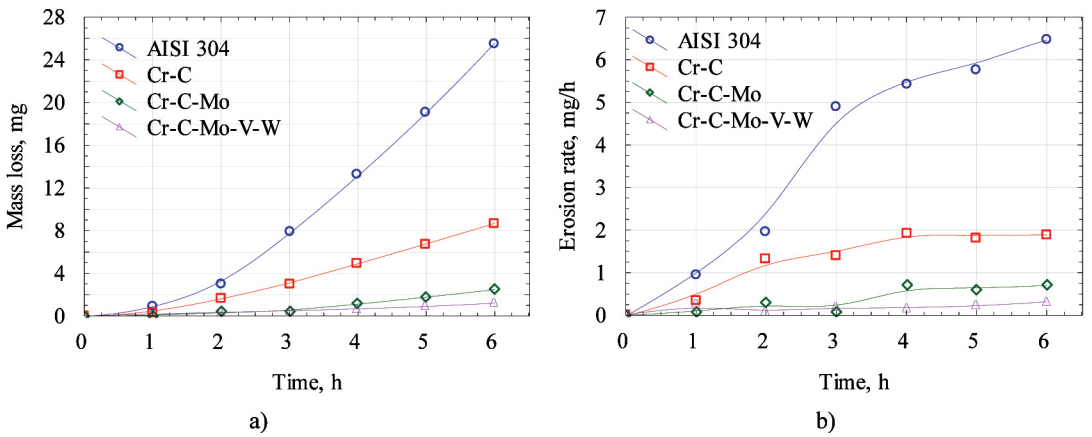

Fig. 3. Results of cavitation erosion testing: a) mass loss; b) erosion rate-time curves
Rys. 3. Rezultaty badań kawitacyjnych: a) ubytek masy; b) krzywe prędkości erozji

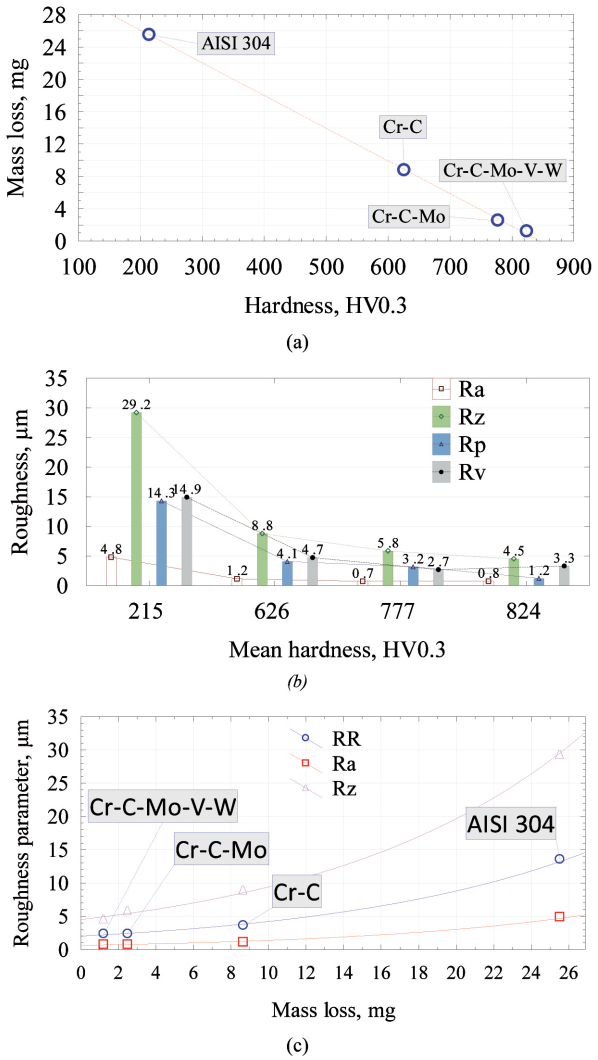

Fig. 4. Effect of hardness on mass loss (a), the plot of multiple roughness parameters against hardness (b) and the relationship between the mass loss and roughness (c) estimated after 6h of erosion testing

Rys. 4. Wpływ twardości na ubytek masy (a), wykres wielu parametrów chropowatości w stosunku do twardości (b) oraz związek między ubytkiem masy a chropowatością (c) oszacowane po 6 godzinach badania erozji

the hardfacings hardness (**Figure 4b**) and pad weld mass losses, **Figure 4c**. Moreover, the proposed roughness rate factor (RR) refers well to material loss. Therefore, the RR provides information about the CE surface damage rate, which has been discussed in the previous paper **[L. 23]** describing the CE resistance of HVOF sprayed coatings.

The visualisation of the eroded surfaces is shown in **Figure 5** and **6**. The profilometric measurements and SEM observations of the damaged surfaces confirm differences in the kinetics of CE process investigated materials. AISI 304 shows a severely roughened surface rich in cavitation pits, plastic deformation and material removal in massive chunks resulting in high Rv and Rp parameters (**Figure 4–6**) which are approximately three times higher than those reported for Cr-C hard facing and four times higher larger than reported for Cr-C-Mo-V-W hard facing (**Figure 4d**). Generally, the roughness profiles are less sharp, showing shallow valleys for harder coatings that withstand well the cavitation loads. The unevenness of the roughness curve refers to the rate of surface erosion.

The erosion mechanism has been identified via SEM observations Figure 6. Contrary to low alloyed steel **[L. 35]**, stainless steel AISI 304 **[L. 16]** and other soft, malleable metal alloys **[L. 22]** which show the ductile mode of CE, in the case of hard weld deposits, brittle mode of erosion mechanism usually dominates **[L. 36]**. The failure mechanism of studied hardfacings shows semi-brittle erosion mode with cracks formation and deformation of the tips of roughened material. Thus, it can be concluded that the fatigue-related cavitation erosion process, combined with the high hardness of hardfacings and multiphase structure, proceeds in brittle-ductile mode, see Figure 6. Cracking is the main deterioration mechanism providing material removal due to the coalescence of cracks initiated in highly deformed regions. Loss of material integrity probably starts at the interfaces of microstructural phases and grain borders. The assessment of the profilometric (**Figure 4** and **5**) and SEM (**Figure 6**) data indicates that surfaces undergo different fragmentation rates. The Cr-C sample shows much coarser chunks of material partition than those reported for the Cr-C-Mo-V-W sample. Moreover, the Cr-C-Mo-V-W surface contains some undamaged areas, as reported by SEM, which slows the rate of roughing and produces relatively uniform roughness profile (**Figure 5d**).

Generally, the differences in chemical composition result in the formation of specific types of phases and characteristic microstructure, i.e., the precipitation of carbides in a martensite matrix. Based on investigations conducted in our previous studies for metal alloys **[L. 10, 18]**, ceramics **[L. 32, 37]** and hard cermet coatings **[L. 8, 38]**, it is claimed that an accurate evaluation of the erosion mechanism must combine the metallographic investigations. Thus, it is suggested that the CE

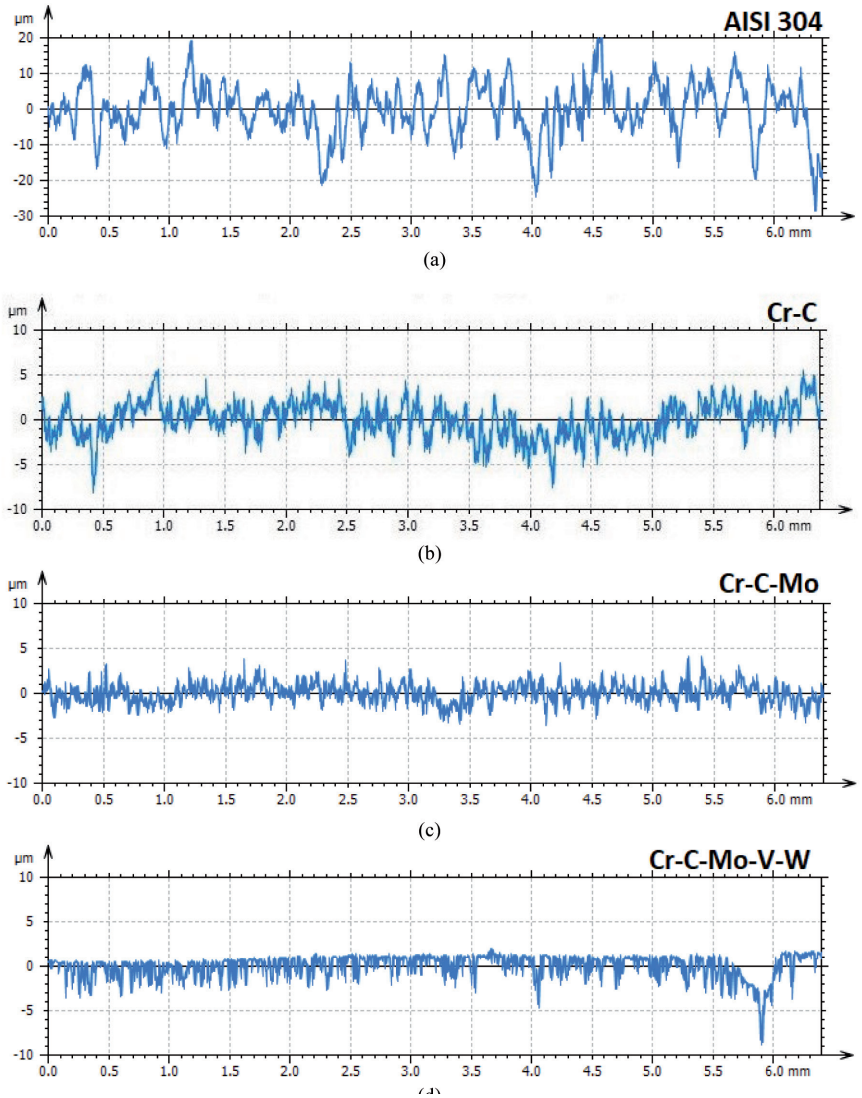

Fig. 5. Roughness profiles visualising roughness valleys and peaks after 6h of exposure to cavitation for: a AISI 304, b) Cr-C, c) Cr-C-Mo, d) Cr-C-Mo-V-W

Rys. 5. Profile chropowatości wizualizujące doliny profili i piki po 6 godzinach ekspozycji na kawitację dla: a) AISI 304, b) Cr-C, c) Cr-C-Mo, d) Cr-C-Mo-V-W

behaviour of hardfacings correlates with the precipitation of carbides in martensite, second-phased content, morphology and distribution microstructure phase. The obtained results for pad welds are very encouraging and reveal the large potential of hard deposits, but because of scarce information in the literature, the effect of hardness and microstructure on CE performance should be refined in further studies. Finally, our study suggests that basic roughness parameters such as Ra, Rz, Rv, Rp etc., can provide satisfying results for CE behaviour description. However, to accurately describe the CE kinetic other types of roughness parameters relating to material ratio curves and probability density curves, stratified functional properties parameters of a surface with stratified functional properties should also be considered.

CONCLUSIONS

The analysis of the cavitation erosion (CE) results obtained for welded hardfacings on structural steel substrate via the SMAW method allows us to draw the following conclusions:

– The Cr-C-Mo-V-W hard facing shows the highest CE resistance and 20 times exceeding the mass loss reported for AISI 304 reference

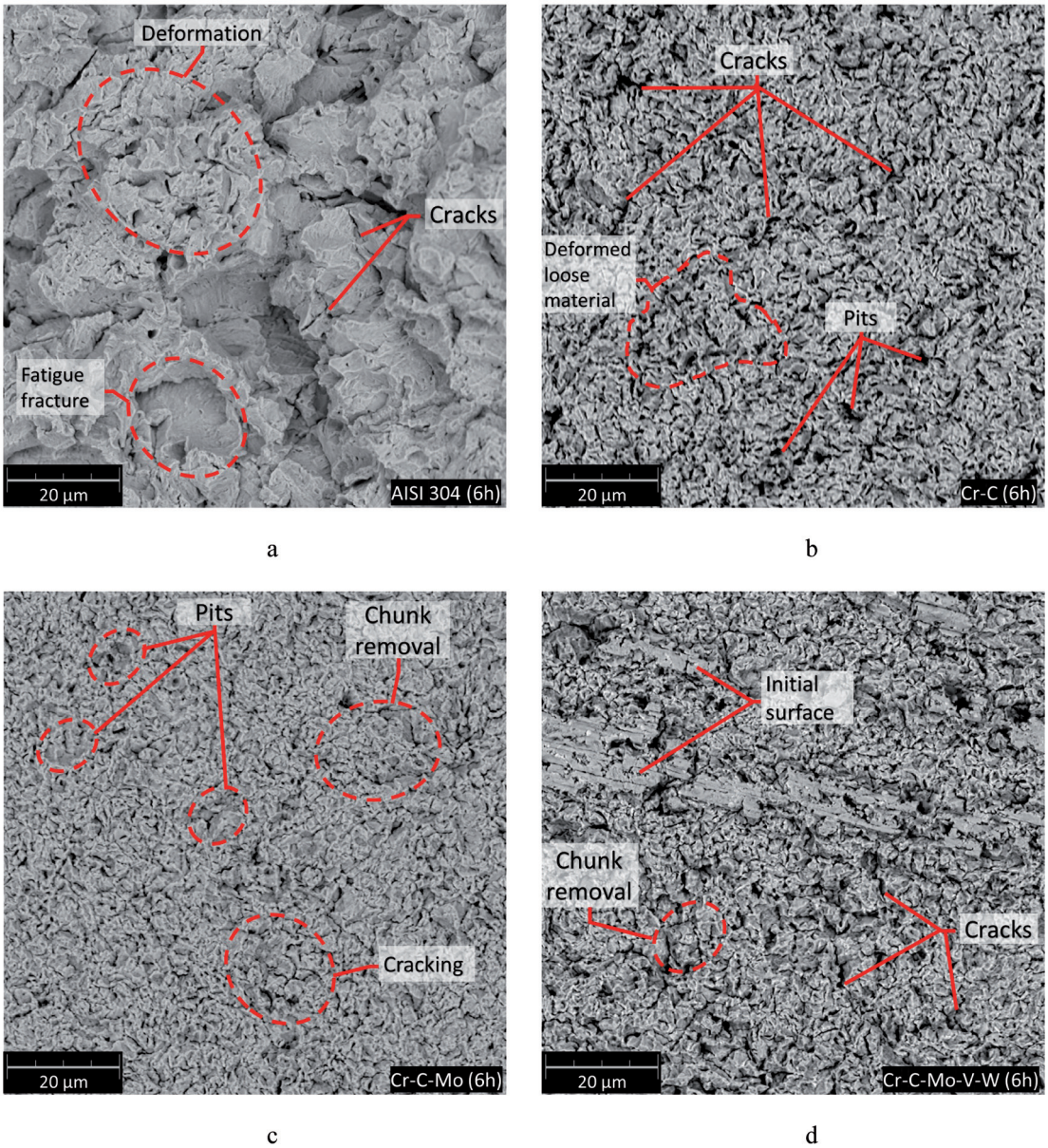

Fig. 6. Hardfacing surfaces after exposure to cavitation erosion: a) AISI 304, b) Cr-C, c) Cr-C-Mo, d) Cr-C-Mo-V-W
Rys. 6. Powierzchnia napoin po badaniach odporności na erozję kawitacyjną: a) AISI 304, b) Cr-C, c) Cr-C-Mo, d) Cr-C-Mo-V-W

steel (25.5 mg). In addition, hardfacings show increased resistance to cavitation erosion in the following order: Cr-C < Cr-C-Mo < Cr-C-Mo-V-W and erosion rates equal 1.92 mg/h, 0.72 mg/h, and 0.32 mg/h, respectively.

– The Cr-C, Cr-C-Mo and Cr-C-Mo-V-W pad welds show hardness of 627HV0.3, 777HV0.3 and 825 HV0.3, respectively, which support the CE resistance of hardfacings.
– In the case of three investigated high-alloyed hardfacings and AISI 304 reference material, increasing material hardness improves resistance to CE. Similarly, the progress of erosive material loss corresponds to the development of Ra, Rz, Rv, and Rp roughness parameters. Finally, the proposed roughness rate (RR) indicator successfully informs about the rate of material damage.
– The erosion mechanism of the coatings can be classified as brittle-ductile and relies on cracking, chunk removal of material, pits and craters formation, and deformation of fractured

material tips and edges. Hardfacings material failed primarily due to brittle fractures with varying severity.
– Detailed microstructure instigations are required to thoroughly explain the effect of alloying elements on microstructure and its impact on the CE behaviour of alloyed ferrous hardfacings.

ACKNOWLEDGEMENT

The project/research was financed in the framework of the project Lublin University of Technology-Regional Excellence Initiative, funded by the Polish Ministry of Science and Higher Education (contract no. 030/RID/2018/19).

REFERENCES

1. Hejwowski T.: Nowoczesne powłoki nakładane cieplnie odporne na zużycie ścierne i erozyjne (Modern wear and erosion resistant thermally deposited coatings). Lublin, Poland: Politechnika Lubelska (Lublin University of Technology), 2013.
2. Kim J.-H., Lee M.-H.: A Study on Cavitation Erosion and Corrosion Behavior of Al-, Zn-, Cu-, and Fe-Based Coatings Prepared by Arc Spraying. J Therm Spray Tech 2010, 19, pp. 1224–30, https://doi.org/10.1007/s11666-010-9521-0.
3. Matikainen V., Koivuluoto H., Vuoristo P.: A study of Cr3C2-based HVOF- and HVAF-sprayed coatings: Abrasion, dry particle erosion and cavitation erosion resistance. Wear 2020, 446–447, p. 203188, https://doi.org/10.1016/j.wear.2020.203188.
4. Szala M., Walczak M., Łatka L., Gancarczyk K., Özkan D.: Cavitation Erosion and Sliding Wear of MCrAlY and NiCrMo Coatings Deposited by HVOF Thermal Spraying. Advances in Materials Science 2020, 20, pp. 26–38, https://doi.org/10.2478/adms-2020-0008.
5. Ding X., Ke D., Yuan C., Ding Z., Cheng X.: Microstructure and Cavitation Erosion Resistance of HVOF Deposited WC-Co Coatings with Different Sized WC. Coatings 2018, 8, p. 307, https://doi.org/10.3390/coatings8090307.
6. Lamana M.S., Pukasiewicz A.G.M., Sampath S.: Influence of cobalt content and HVOF deposition process on the cavitation erosion resistance of WC-Co coatings. Wear 2018, 398–399 pp. 209–19, https://doi.org/10.1016/j.wear.2017.12.009.
7. Liu J., Bai X., Chen T., Yuan C.: Effects of Cobalt Content on the Microstructure, Mechanical Properties and Cavitation Erosion Resistance of HVOF Sprayed Coatings. Coatings 2019, 9, p. 534, https://doi.org/10.3390/coatings9090534.
8. Jonda E., Szala M., Sroka M., Łatka L., Walczak M.: Investigations of cavitation erosion and wear resistance of cermet coatings manufactured by HVOF spraying. Applied Surface Science 2023, 608, p. 155071, https://doi.org/10.1016/j.apsusc.2022.155071.
9. Oliveira D.B., Franco A.R., Bozzi A.C.: Influence of low temperature plasma carbonitriding on cavitation erosion resistance of the Stellite 250 alloy – A preliminary evaluation. Wear 2021, p. 203653, https://doi.org/10.1016/j.wear.2021.203653.
10. Szala M., Chocyk D., Skic A., Kamiński M., Macek W., Turek M.: Effect of Nitrogen Ion Implantation on the Cavitation Erosion Resistance and Cobalt-Based Solid Solution Phase Transformations of HIPed Stellite 6. Materials 2021, 14, p. 2324, https://doi.org/10.3390/ma14092324.
11. Krella A., Marchewicz A.: Effect of mechanical properties of CrN/CrCN coatings and uncoated 1.402 stainless steel on the evolution of degradation and surface roughness in cavitation erosion. Tribology International 2023, 177, https://doi.org/10.1016/j.triboint.2022.107991.
12. Díaz V.V., Dutra J.C., Buschinelli A.J. de A, D'Oliveira A.S.C.: Cavitation erosion resistance of deposits processed by plasma transferred arc welding. Welding International 2009, 23, pp. 159–65, https://doi.org/10.1080/09507110802543286.

13. Hattori S., Mikami N.: Cavitation erosion resistance of stellite alloy weld overlays. Wear 2009, 267, pp. 1954–60, https://doi.org/10.1016/j.wear.2009.05.007.
14. Will C.R., Capra A.R., Pukasiewicz A.G.M., Chandelier J. da G., Paredes R.S.C.: Comparative study of three austenitic alloy with cobalt resistant to cavitation deposited by plasma welding. Welding International 2012, 26, pp. 96–103, https://doi.org/10.1080/09507116.2010.527487.
15. Zhao T., Zhang S., Wang Z.Y., Zhang C.H., Zhang D.X., Wang N.W., et al.: Cavitation erosion/corrosion synergy and wear behaviors of nickel-based alloy coatings on 304 stainless steel prepared by cold metal transfer. Wear 2022, 510–511, p. 204510, https://doi.org/10.1016/j.wear.2022.204510.
16. Szala M., Walczak M., Hejwowski T.: Factors Influencing Cavitation Erosion of NiCrSiB Hardfacings Deposited by Oxy-Acetylene Powder Welding on Grey Cast Iron. Adv Sci Technol Res J 2021, 15, pp. 376–86, https://doi.org/10.12913/22998624/143304.
17. Duraiselvam M., Galun R., Wesling V., Mordike B.L., Reiter R., Oligmüller J.: Cavitation erosion resistance of AISI 420 martensitic stainless steel laser-clad with nickel aluminide intermetallic composites and matrix composites with TiC reinforcement. Surface and Coatings Technology 2006, 201, pp. 1289–95, https://doi.org/10.1016/j.surfcoat.2006.01.054.
18. Szymański Ł., Olejnik E., Sobczak J.J., Szala M., Kurtyka P., Tokarski T., et al.: Dry sliding, slurry abrasion and cavitation erosion of composite layers reinforced by TiC fabricated in situ in cast steel and gray cast iron. Journal of Materials Processing Technology 2022, 308, p. 17688, https://doi.org/10.1016/j.jmatprotec.2022.117688.
19. Fedorov A.V., Rymkevich A.I., Bazhenov V.V., Zubchenko A.S., Davydova N.V.: Cavitation-resistant high-alloyed chromium steels. Welding International 2015, 29, pp. 894–900, https://doi.org/10.1080/09507116.2014.998432.
20. ESAB Welding Handbook. Consumables for Manual and Automatic Welding Consumables for Hardfacing 2005, https://www.academia.edu/35539666/ESAB_WELDING_HANDBOOK (accessed October 31, 2022).
21. ASTM G32-16 Standard Test Method for Cavitation Erosion Using Vibratory Apparatus 2016, https://doi.org/10.1520/G0032-16.
22. Szala M., Łatka L., Walczak M., Winnicki M.: Comparative Study on the Cavitation Erosion and Sliding Wear of Cold-Sprayed Al/Al2O3 and Cu/Al2O3 Coatings, and Stainless Steel, Aluminium Alloy, Copper and Brass. Metals 2020, 10m p. 856, https://doi.org/10.3390/met10070856.
23. Szala M.: Cavitation erosion phenomenological model of MCrAlY and NiCrMoNbTa metallic coatings deposited via the HVOF method. Tribologia 2021, 298 pp. 47–55, https://doi.org/10.5604/01.3001.0015.8368.
24. Rakhit A.K.: Heat Treatment of Gears: A Practical Guide for Engineers. Materials Park, OH: ASM International, 2000.
25. Drozd K., Walczak M., Szala M., Gancarczyk K.: Tribological Behavior of AlCrSiN-Coated Tool Steel K340 Versus Popular Tool Steel Grades. Materials 2020, 13, p. 4895, https://doi.org/10.3390/ma13214895.
26. Sawa M., Szala M., Henzler W.: Innovative device for tensile strength testing of welded joints: 3d modelling, FEM simulation and experimental validation of test rig – a case study. Applied Computer Science 2021, 17, pp. 92–105, https://doi.org/10.23743/acs-2021-24.
27. Zheng Y., Wang F., Li C., Lin Y., Cao R.: Effect of Martensite Structure and Carbide Precipitates on Mechanical Properties of Cr-Mo Alloy Steel with Different Cooling Rate. High Temperature Materials and Processes 2019, 38, pp. 113–24, https://doi.org/10.1515/htmp-2018-0018.
28. He X., Hu C., Wang Z., Zhao H., Wei X., Dong H.: Carbide transformation behaviors of a Cr–Mo–V secondary hardening steel during over-ageing. Mater Res Express 2020, 7, 036511, https://doi.org/10.1088/2053-1591/ab7c86.
29. Fan C., Chen M.-C., Chang C.-M., Wu W.: Microstructure change caused by (Cr,Fe)23C6 carbides in high chromium Fe–Cr–C hardfacing alloys. Surface and Coatings Technology 2006, 201, pp. 908–12, https://doi.org/10.1016/j.surfcoat.2006.01.010.
30. Hattori S., Ishikura R., Zhang Q.: Construction of database on cavitation erosion and analyses of carbon steel data. Wear 2004, 257, pp. 1022–9, https://doi.org/10.1016/j.wear.2004.07.002.

31. Hattori S., Ishikura R.: Revision of cavitation erosion database and analysis of stainless steel data. Wear 2010, 268, pp. 109–16, https://doi.org/10.1016/j.wear.2009.07.005.
32. Nowakowska M., Łatka L., Sokołowski P., Szala M., Toma F.-L., Walczak M.: Investigation into microstructure and mechanical properties effects on sliding wear and cavitation erosion of Al2O3–TiO2 coatings sprayed by APS, SPS and S-HVOF. Wear 2022, p. 204462, https://doi.org/10.1016/j.wear.2022.204462.
33. Szala M., Walczak M., Świetlicki A.: Effect of Microstructure and Hardness on Cavitation Erosion and Dry Sliding Wear of HVOF Deposited CoNiCrAlY, NiCoCrAlY and NiCrMoNbTa Coatings. Materials 2022, 15, p. 93, https://doi.org/10.3390/ma15010093.
34. Szala M., Chocyk D., Turek M.: Effect of manganese ion implantation on cavitation erosion resistance of HIPed Stellite 6. Acta Physica Polonica A 2022, 142, in print, https://doi.org/10.12693/.
35. Krella A.K., Zakrzewska D.E., Marchewicz A.: The resistance of S235JR steel to cavitation erosion. Wear 2020, 452–453, p. 203295, https://doi.org/10.1016/j.wear.2020.203295.
36. Santa J.F., Blanco J.A., Giraldo J.E., Toro A.: Cavitation erosion of martensitic and austenitic stainless steel welded coatings. Wear 2011, 271, pp. 1445–53, https://doi.org/10.1016/j.wear.2010.12.081.
37. Szala M., Kamiński M., Łatka L., Nowakowska M.: Cavitation erosion and wet environment tribological behavior of Al2O3-13% TiO2 coatings deposited via different atmospheric plasma spraying parameters. Acta Physica Polonica A 2022, 142, in print, https://doi.org/10.12693/.
38. Szala M., Dudek A., Maruszczyk A., Walczak M., Chmiel J., Kowal M.: Effect of atmospheric plasma sprayed TiO2-10% NiAl cermet coating thickness on cavitation erosion, sliding and abrasive wear resistance. Acta Phys Pol A 2019, 136, pp. 335–41, https://doi.org/10.12693/APhysPolA.136.335.